THE ASTROPHYSICAL JOURNAL, 448:L77–L80, 1995 August 1

SPECTROPOLARIMETRY OF TWO BROAD ABSORPTION LINE QUASARS WITH THE W. M. KECK TELESCOPE

M. H. COHEN, P. M. OGLE, H. D. TRAN, AND R. C. VERMEULEN
Palomar Observatory, California Institute of Technology, Pasadena, CA 91125

AND

J. S. MILLER, R. W. GOODRICH,[1] AND A. R. MARTEL
UCO/Lick Observatory, University of California, Santa Cruz, CA 95064
Received 1995 January 30; accepted 1995 May 18

ABSTRACT

We have observed the broad absorption line quasars PHL 5200 and 0105−265 with spectropolarimetry at the Keck telescope. In PHL 5200 the continuum is consistent with a power law with constant polarization, $p = 5.1\%$. A drop in polarization in the red is explained with dilution by unpolarized Fe II emission. In both objects the permitted emission lines are unpolarized. In PHL 5200 the semiforbidden line C III] λ1909 is weakly polarized; we attribute this to resonance scattering. The polarization rises in the broad absorption troughs, to a peak of 12% in both objects. The high values of p are restricted to a narrow velocity range that is well inside the absorption troughs. In each object, the polarization position angle is constant, except that in PHL 5200 there are marginally significant rotations in the C IV trough and in the C III] emission line. We describe two simple geometries that can explain some of these features. In the first, there are scattered and direct rays; in the troughs the direct ray (unpolarized) is largely absorbed, and we mainly see the highly polarized scattered ray. In the other, the high trough polarization is caused by resonance scattering.

Subject headings: polarization — quasars: absorption lines — quasars: emission lines — quasars: individual (PHL 5200, 0105−265)

1. INTRODUCTION

The broad absorption line (BAL) quasars provide important clues to our understanding of quasars, especially concerning the geometry and motions of various clouds around the nucleus. We have observed two of these objects, PHL 5200 and 0105−265, with the Keck telescope in its spectropolarimetric mode. In this Letter we present the observational results, and describe two simple scenarios which can explain them. These results confirm and extend earlier spectropolarimetry on BAL quasars: PHL 5200 (Stockman, Angel, & Hier 1981; Goodrich & Miller 1995) and CSO 755 (Glenn, Schmidt, & Foltz 1994).

The observations were made at the Keck telescope with a new dual-beam polarimeter, which will be described in a separate paper. The polarimeter was installed directly under the slit of the Low Resolution Imaging Spectrometer (Oke et al. 1995). The seeing was 1″ or better. We used a long slit 1″ wide, a 300 g mm^{-1} grating, blazed at 5000 Å, and a CCD chip with 2048 × 2048 15 μm pixels, giving a dispersion of 2.49 Å pixel^{-1}. The resolution was ~12 Å. No filters were used, and above ~7500 Å the data possibly are contaminated by second-order blue light. This effect is small, at most a few percent of the total intensity.

The BAL quasars PHL 5200 and 0105−265 were observed on 1994 August 3 and October 28, and 0105−265 was observed again on 1994 November 6, giving a total exposure of 2 hr on PHL 5200 and 3 hr on 0105−265. The fluxes were calibrated with GD 248 and Feige 34. To determine the Stokes parameters we made sets of four 900 s exposures with the half-wave plate set at position angles 0°, 45°, 22°.5 and 67°.5, and calculated I, Q, and U in the usual way. Data from the different epochs were binned to 5 Å per bin and co-added. We made no attempt to correct for interstellar polarization, since PHL 5200 and 0105−265 are at high Galactic latitudes (−50° and −86°, respectively).

[1] Current address: Space Telescope Science Institute, 3700 San Martin Drive, Baltimore, MD 21218

2. RESULTS

2.1. *PHL 5200*

Figures 1*a* and 1*b* give spectra of the flux F_λ and the polarization position angle P.A. = 0.5 arctan (u/q) (u and q are normalized Stokes parameters). The P.A. spectrum is nearly constant at P.A. = 163°, and we rotate the (q, u) axes by 326° to obtain an estimate of the fractional linear polarization, p, shown in Figure 1*c*. Since we only have small angular errors Δ(P.A.) (at most 10°), the bias factor cos 2Δ(P.A.) of this estimator is close to unity and using it probably introduces less error than estimating the polarization as $(q^2 + u^2)^{1/2}$ with an appropriate correction algorithm (Simmons & Stewart 1985). Figure 1*d* shows the "total flux" F_λ superposed on pF_λ, the "polarized flux," with relative scales chosen to match the continua at 5000 Å. The important features are as follows.

2.1.1. *Emission Lines*

The emission lines do not appear in pF_λ (Fig. 1*d*), except for C III]. Subtraction of smooth continua in I, Q, and U gives p(C III]) = 1.3 ± 0.3%, and the P.A. may be different from that in the continuum: P.A.(C III]) = 150° ± 5°. The other lines have a polarization consistent with zero; the strongest, C IV, has $p < 0.4\%$.

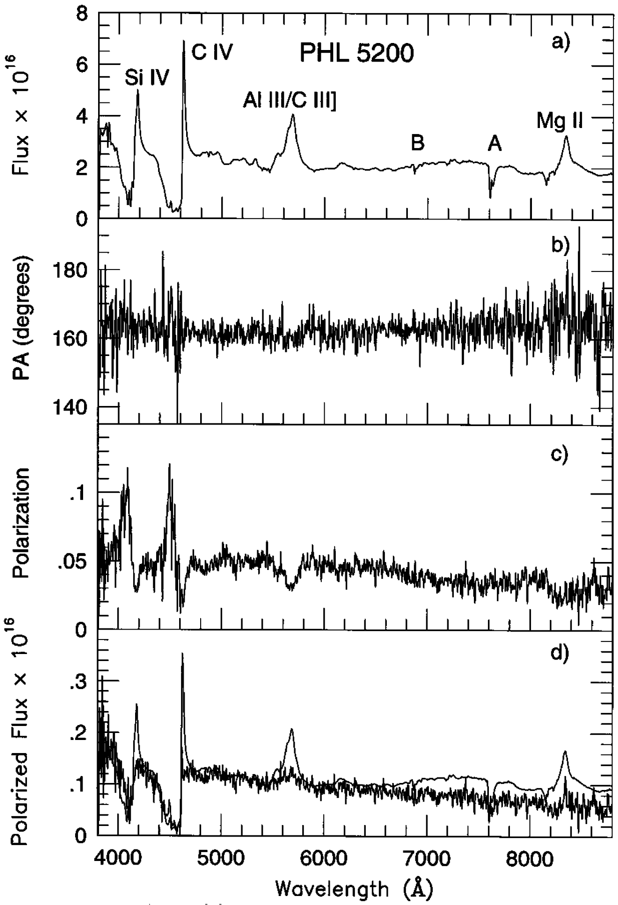

FIG. 1.—PHL 5200 (*a*) Total flux F_λ (*b*) Polarization position angle (*c*) Fractional linear polarization *p* (*d*) 0.051 × F_λ superposed on pF_λ. In (*a*) and (*d*) the telluric bands due to oxygen and water have not been removed.

2.1.2. *Continuum and* Fe II

Except for the absorption troughs, *p* (Fig. 1*c*) is highest between the C IV and Al III emission features, where it may be least contaminated by emission lines. We define p_c as the "continuum" polarization and, averaged over 5015–5497 Å, $p_c = 5.1 \pm 0.1\%$. Between the C III] and Mg II emission lines *p* decreases to 3%, while the total flux (Fig. 1*a*) shows a broad bump. The product pF_λ (Fig. 1*d*) is smooth in this spectral region, and, redward of the C IV absorption trough, can be approximated by a power law with index $\alpha = -0.9 \pm 0.1$ ($pF_\nu \propto \nu^\alpha$) (apart from the C III] emission feature and a possible feature at Mg II). Figure 1*d* also shows $p_c F_\lambda$. The excess of $p_c F_\lambda$ over pF_λ strongly resembles Fe II emission (see, e.g., the composite quasar spectrum by Francis et al. 1991), and so we suggest that the drop in *p* redward of C III] is due to dilution by unpolarized Fe II emission. The drop in polarization to the red is also noted by other authors (Stockman et al. 1981; Goodrich & Miller 1995), who suggest other dilution mechanisms, or a wavelength-dependent opacity effect. Wills et al. (1992), in commenting on the Stockman et al. data, also suggested that the drop in *p* in PHL 5200 could be due to dilution by unpolarized Fe II emission.

2.1.3. *The Troughs*

The polarization in the C IV trough (Fig. 2*c*) has a peak $p_{max} \sim 12\%$, near -8000 km s^{-1}. The region where $p > p_c$ is substantially narrower than the trough in F_λ, and $p < p_c$ from roughly +5000 to -3000 km s^{-1}. On the blue side, *p* falls to p_c at about $-14{,}000$ km s^{-1}. The Si IV trough is weaker than the C IV trough, but has similar polarization, with $p_{max} \sim 11\%$ near -6000 km s^{-1}.

In PHL 5200 the P.A. (Fig. 2*b*) rotates between -6600 and -7900 km s^{-1}, with a peak of 175° near -6900 km s^{-1}. This velocity range covers 4 pixels, and when averaged appropriately the ~10° shift in P.A. is a 3 σ result. We have at most a marginal detection of a P.A. change, but lending support to its reality is the bump in F_λ and in pF_λ in the same velocity range. Turnshek et al. (1988) emphasize this peak, which is designated region c-d in their Figure 7.

2.2. *0105−265*

Figure 3 shows spectra for 0105−265. The continuum flux and polarization are both less than in PHL 5200, and the noise in *p* is correspondingly greater. The P.A. (Fig. 3*b*) is almost constant with wavelength, at 138°, and we rotate the (*q*, *u*) axes by 276° to obtain an estimate for *p*, shown in Figure 3*c*. Figure 3*d* shows the SNR in *p*, calculated from photon statistics. Read noise and systematic errors due to sky subtraction are small. Note that the SNR is not appreciably worse in the troughs than in the neighboring continuum, since the fall in F_λ is compensated by the rise in *p*.

The continuum between the main absorption and emission features has $p_c \sim 2\%$. As with PHL 5200, the polarization is

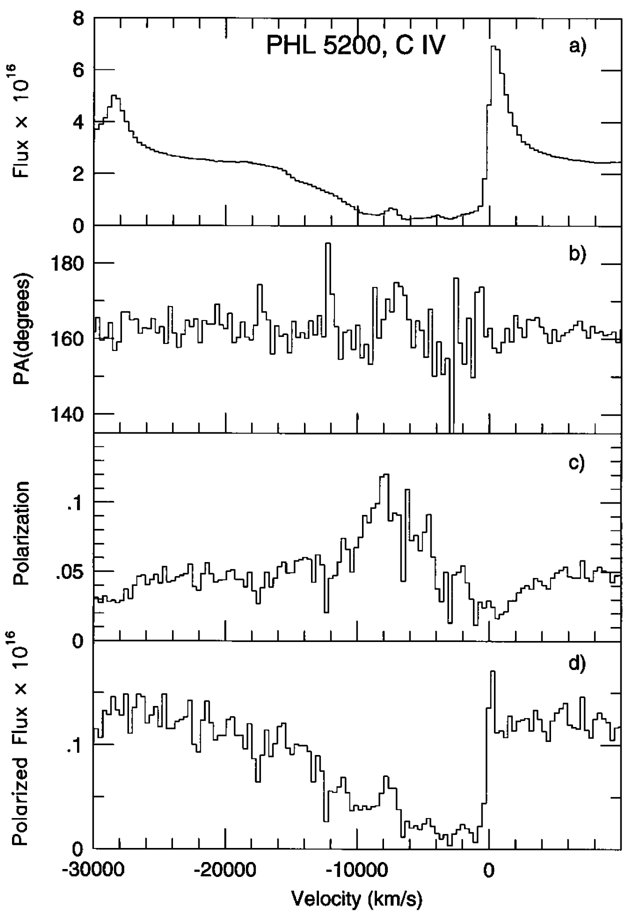

FIG. 2.—The C IV region for PHL 5200. (*a*) Total flux F_λ. (*b*) Polarization position angle. (*c*) Fractional linear polarization *p*. (*d*) Polarized flux pF_λ.

clearly reduced in the emission lines O VI, Lyα/N V and C IV, and, less convincingly, in Si IV and C III]; and it shows strong increases in the absorption troughs due to C IV, S IV, Lyα/N V, O VI, and a 3 σ increase in S VI. The polarized flux pF_λ shows a decrease in the absorption troughs of C IV and N V/Lyα and a noisy but real decrease in the troughs of Si IV and O VI. The emission lines are not evident in pF_λ, and the upper limit to p depends critically on the determination of the neighboring continuum. A conservative estimate for Lyα/N V is $p < 0.5\%$.

In 0105−265 the contrast in p between the trough and the continuum is striking. Although the continuum polarization is less than half that in PHL 5200, the two quasars have similar values of $p_{\rm max}$ in the C IV trough. In both objects the maximum lies blueward of the center of the deep portion of the trough, and on the blue side p falls to p_c where F_λ is still near its minimum.

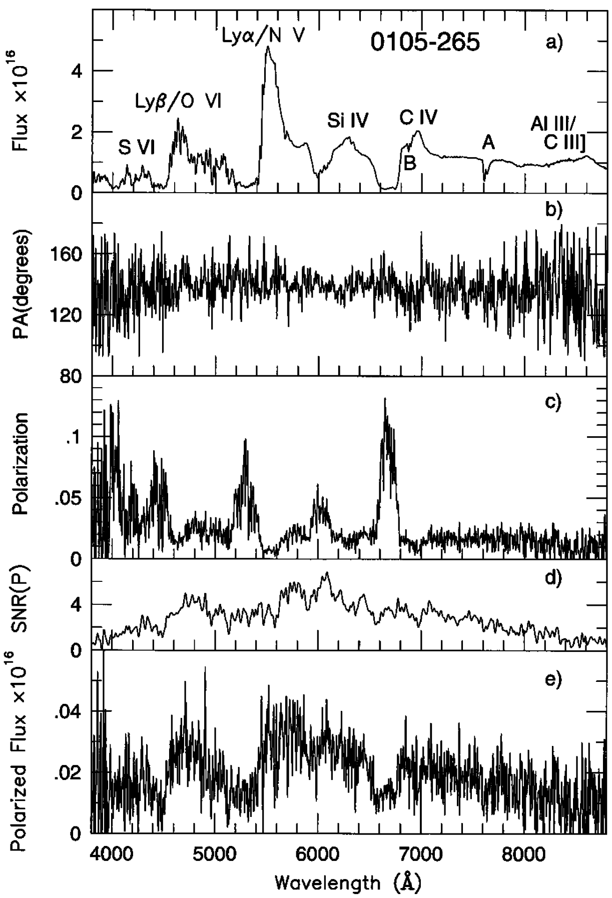

FIG. 3.—0105−265 (*a*) Total flux F_λ (*b*) Polarization position angle (*c*) Fractional linear polarization p (*d*) SNR = $p/\sigma(p)$ (*e*) Polarized flux pF_λ.

3. DISCUSSION

These observations with the Keck telescope provide substantially greater sensitivity than has previously been available, and they show that the polarization structure in BAL quasars is complex. We now briefly discuss the polarization and consider two simple geometric models.

3.1. *Continuum*

We suggest in § 2.1 that the radiation from PHL 5200 contains a continuum component whose spectrum is close to a smooth power law with $\alpha = -0.9$, that this component has a polarization $p_c \geq 5.1\%$ independent of wavelength, and that the decrease in p redward of C III] is due to dilution by unpolarized Fe II emission. If the continuum polarization is indeed wavelength independent, the scattering is probably caused by electrons; however, approximate wavelength independence can also be produced by dust. Synchrotron radiation is less likely because this is typically associated with radio-loud objects, whereas BAL quasars are all radio quiet (Stocke et al. 1992).

The spectrum of 0105−265 does not extend beyond C III], but between C IV and C III] the index of pF_ν is $\alpha \sim +0.7$. For comparison, the polarized flux in CSO 755 has $\alpha = -0.4 \pm 0.3$ (Glenn et al. 1994). The polarized flux in BAL quasars clearly has a wide range of spectral indices, as does the UV flux in radio-quiet quasars generally (Francis et al. 1991).

3.2. *Emission Lines*

The C III] emission in PHL 5200 is clearly polarized, at ~1.3%, whereas the other broad emission lines in both objects show no evidence of polarization. Our observation agrees with the theoretical predictions of Lee, Blandford, & Western (1994) and Lee (1994), who calculated the polarization expected from resonantly scattered photons in the BELR. Significant polarization requires a modest optical depth (of order 1–10) to resonance scattering, which could be satisfied by the semiforbidden C III] line but not by the permitted lines.

Our measurements confirm the marginal detection of C III] polarization by Goodrich & Miller (1995) and the earlier result by Stockman et al. (1981) that the emission lines are generally unpolarized. Stockman et al. also reported p(C III]) = 0.4 ± 1.6%, which is consistent with our result. Glenn et al. (1994) showed that the permitted lines in CSO 755 are unpolarized; their data did not extend to C III].

3.3. *BAL Troughs*

In both objects, the polarization in the C IV troughs has a narrow peaked shape, with a maximum blueward of the center of the deep troughs. In PHL 5200 the trough is not detached, and we suggest that the reduction in p below p_c from 0 to −3000 km s^{-1} is due to dilution by the blue wing of the unpolarized C IV line. In support of this we note in Figure 2 that from about −500 to −3000 km s^{-1} p rises by a factor of 2 while F_λ falls by the same factor, and pF_λ is constant, to within noise.

The troughs show striking wavelength-dependent phenomena that must be connected with the detailed structure of the BALR. Resonance scattering probably is producing some of the polarization structure, and wavelength-dependent dilution is another possibility. We now discuss two simple geometric models in which these effects appear separately.

3.4. *Geometric Models*

Weymann et al. (1991) showed that BAL quasars probably are just a subset of all radio-quiet quasars, those which happen to be seen through a broad absorption line region. Since ~12% of quasars show broad absorption lines, the BALR must cover ~12% of the solid angle around the central region. Weymann et al. also suggested that the BAL clouds are driven off an equatorial disk, so that a BAL quasar is always viewed near the equator. We adopt this picture also.

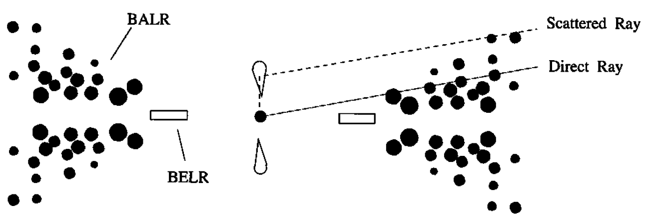

FIG. 4.—A schematic diagram of the absorbing and scattering regions in a BAL quasar. The scattered lines of sight are farther from the equatorial plane than is the direct line of sight and have a lower optical depth in the BALR.

3.4.1. *Scattering on the Axis*

Figure 4 shows a schematic model in which the high polarization in the troughs comes from reduced dilution. A scattering region lies on the axis. The scattered continuum contains most of the polarization and is diluted by the direct ray, but less at wavelengths where the latter is heavily absorbed. The scattered ray must go through a weakened BALR at low velocities, since the absorption is less in pF_λ than in F_λ. At high velocities, however, the direct and scattered rays have the same optical depth. (See Fig. 2*c*; $p \simeq p_c$ for $v < -14{,}000$ km s^{-1}.) The possible P.A. rotation near -6900 km s^{-1} in PHL 5200 is not explained in this picture, since, if real, it requires another polarized component.

The emission lines give three constraints. First, the BELR must be occulted by the BALR, which cuts off the blue wing of C IV in PHL 5200 (see Fig. 2; for details, see Turnshek et al. 1988). Figure 4 is not to be taken literally, but it indicates that on near-equatorial lines of sight the radiation from the BELR passes through the BALR. Second, C III] is weakly polarized, and in § 3.2, we suggest that this is due to resonant scattering in the BELR. The third constraint is that the permitted lines are polarized much less than the continuum. This can be satisfied, for example, if the size of the BELR is comparable with or greater than that of the scattering region. The possible P.A. rotation of C III] is readily explained: the continuum is polarized nearly perpendicular to the axis, but the P.A. of the resonantly scattered light depends on the detailed geometry of the BELR.

3.4.2. *Resonance Scattering*

An alternative view of the high polarization in the troughs is that it is due to resonance scattering in the BALR. Figure 4 can represent this case if we eliminate the scattering region and the scattered ray. The continuum now is intrinsically polarized 5.1%, perhaps by scattering in a small disk around the nucleus, and the continuum P.A. is controlled by the optical depth in the disk. (Phillips & Mészáros 1986). The C III] emission is again polarized by resonance scattering in the BELR.

The wavelength dependence of the resonantly scattered light for disk and cone models has been calculated by Hamann, Korista, & Morris (1993), and the polarization characteristics are calculated by Lee & Blandford (1995). Our measured peak polarization, 12%, seen in the C IV and Si IV troughs, is comparable with the peak values obtained by Lee & Blandford for an equatorial flow. This mechanism can be at least partly responsible for the trough polarization. A problem with the model is that it predicts extra polarized light in the red wings of the emission lines, but so far this has not been seen.

If the P.A. rotation in the C IV trough of PHL 5200 is real, it could mean that two polarization mechanisms are at work. A combination of electron scattering and resonance scattering in the BALR, together with appropriate variations in optical depth, may be able to explain it. It will be important to confirm or deny this tentative result, and to measure the rotation with precision if it does exist.

We are grateful to Walter Schaal, who did most of the engineering work on the polarimeter, and to Tom Bida and others at the W. M. Keck Observatory for their assistance. We thank Vino Vats and the Karl Lambrecht Company, for their exceptional efforts in producing the beamsplitter. We have benefited greatly from discussions with R. Blandford, H. Lee, and R. Weymann, and from comments by B. Wills and by an anonymous referee.

The W. M. Keck Observatory is operated as a scientific partnership between the California Institute of Technology and the University of California. It was made possible by the generous financial support of the W. M. Keck Foundation. This work was supported, in part, by NSF grants AST-9121889 and AST-9117100.

REFERENCES

Francis, P. J., Hewett, P. C., Foltz, C. B., Chaffee, F. H., Weymann, R. J., & Morris, S. L. 1991, ApJ, 373, 465
Glenn, J., Schmidt, G. D., & Foltz, C. B. 1994, ApJ 434, L47
Goodrich, R. W., & Miller, J. S. 1995, ApJ, 448, L73
Hamann, F., Korista, K. T., & Morris, S. L. 1993, ApJ, 415, 541
Lee, H. W., 1994, MNRAS, 268, 49
Lee, H. W., & Blandford, R. D. 1995, in preparation
Lee, H. W., Blandford, R. D., & Western, L. 1994, MNRAS 267, 303
Oke, J. B., et al. 1995, PASP, 107, 375
Phillips, K. C., & Mészáros, P. 1986, ApJ, 310, 284
Simmons, J. F. L., & Stewart, B. G. 1985, A&A, 172, L11
Stocke, J. T., Morris, S. L., Weymann, R. J., & Foltz, C. B. 1992, ApJ, 396, 487
Stockman, H. S., Angel, J. R. P., & Hier, R. G. 1981, ApJ, 243, 404
Turnshek, D. A., Foltz, C. B., Grillmair, C. J., & Weymann, R. J. 1988, ApJ, 325, 651
Weymann, R. J., Morris, S. L., Foltz, C. B., & Hewett, P. C. 1991, ApJ, 373, 23
Wills, B. J., Wills, D., Evans, N. J., Natta, A., Thompson, K. L., Breger, M., & Sitko, M. L. 1992, ApJ, 400, 96